Modeling of Velocity-Field Characteristics in Strained Silicon

S. Dhar, G. Karlowatz, E. Ungersboeck, H. Kosina, and S. Selberherr

Institute for Microelectronics, TU Wien, Gußhausstraße 27–29, 1040 Wien, Austria
E-mail: dhar@iue.tuwien.ac.at

ABSTRACT

We have performed a detailed analysis of the electron transport at high electric field in strained Si for different field directions and stress/strain conditions using full-band Monte Carlo simulations. A model describing the velocity-field relationship for biaxially or uniaxially strained Si has been developed.

INTRODUCTION

Uniaxially strained Si offering larger electron and hole mobilities [1] [2] compared to conventional Si is becoming increasingly accepted by the semiconductor manufacturing industry. The superior transport properties delivered due to strain stem from an alteration of the band structure by lifting the degeneracy in both the conduction and valence bands. In the conduction band the Δ_6-valleys are split into 2-fold degenerate Δ_2-valleys and 4-fold degenerate Δ_4-valleys. A negative energy splitting ($\Delta\epsilon = \Delta_2 - \Delta_4$) results in reduced inter-valley phonon scattering as well as a lower effective mass in transport direction. The enhancement of the low-field electron mobility in strained Si has been modeled in [3]. The model describes the mobility tensor for electrons in strained Si as a function of $\Delta\epsilon$. The present work examines the electron high-field transport in strained Si using Monte Carlo (MC) simulations. A strain dependent empirical model describing the longitudinal velocity component as a function of the magnitude and direction of the electric field is presented.

MONTE CARLO RESULTS

The band structure for strained Si was calculated using the empirical pseudopotential method [4]. Fig. 1 and Fig. 2 show the velocity-field characteristics as obtained from full-band MC simulations for biaxially strained Si grown on a relaxed SiGe [001] substrate for different Ge content and field along in-plane ([100]) and out-of-plane ([001]) directions, respectively. The figures show an increase (decrease) in the electron velocity with increasing strain for field along [100] ([001]) direction. For a field along the in-plane direction, the electron velocity shows a region of small negative differential mobility. The velocity-field characteristics shown in Fig. 2 exhibit an non-typical form for high strain levels. This curve is associated with the Δ_2-valleys which move down in energy with increasing strain and have the longitudinal

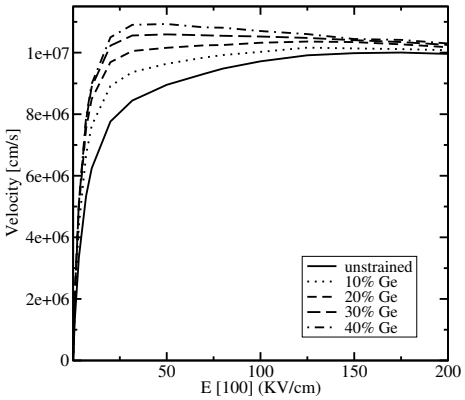

Figure 1: Electron velocity versus field (along [100]) in strained Si on SiGe with increasing Ge content obtained from MC simulations.

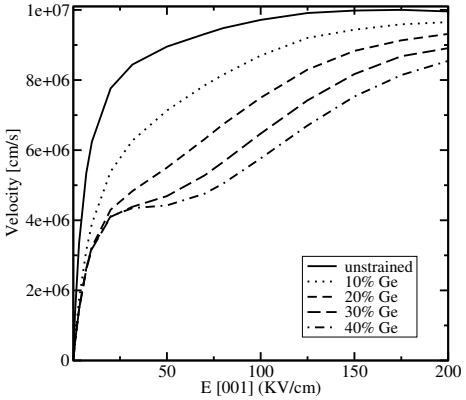

Figure 2: Electron velocity versus field (along [001]) in strained Si on SiGe with increasing Ge content obtained from MC simulations.

mass in the field direction. Repopulation effects within this 2-fold degenerate valley together with a high population lead to the particular shape of the velocity-field curve.

HIGH FIELD MODEL

The high field behavior is modeled using direct fits of empirical expressions to the MC data. We have restricted our study to strain conditions where only one pair of X-valleys is shifted with respect to the four-fold degenerate X-valleys. These conditions include biaxial stress and uniaxial stress applied along the principal axes of the crystal ({100} directions for Si). The velocity along the field direction is modeled phenomenologically using the expression

$$v(E) = \frac{2\mu_0 E}{1 + \left[1 + \left(\frac{2\mu_0 E}{v_s(1-\xi)}\right)^{\beta}\right]^{1/\beta}} + v_s \xi \frac{(E/E_0)^{\gamma}}{1 + (E/E_0)^{\gamma}}, \tag{1}$$

which is an extension of the standard mobility model used in [5]. Here μ_0 is the low field mobility and v_s is the saturation velocity. Any velocity component perpendicular to the field direction is not considered in this work, so that a simple, scalar mobility model $\mu(E) = v(E)/E$, is obtained. The additional term incorporated in (1) models the velocity kink shown in Fig. 2. E_0 and γ are fit parameters. The empirical dependences of the parameters v_s, β, E_0 and γ are described using linear functions of $\Delta\epsilon$. The parameter ξ is modeled by a rational expression.

$$\xi = \frac{(\Delta\epsilon/\xi_0)}{1 + (\Delta\epsilon \cdot \xi_1/\xi_0)^2} \tag{2}$$

Fig 3 shows the typical variation of the parameters v_s, β and ξ for uniaxially stressed Si for [001], [100] and [110] field directions. The coefficients for the linear expressions as well as those in (2) are constants for a particular field direction and have been obtained using the optimization framework of MATLAB. Fig. 4 shows the velocity-

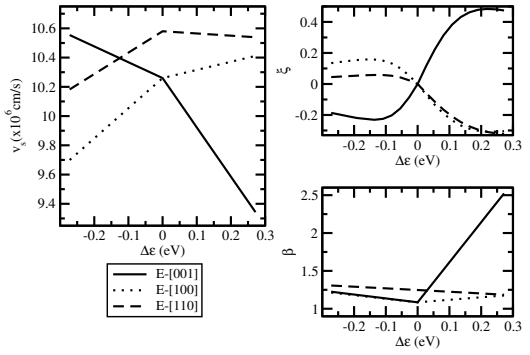

Figure 3: Variation of parameters with strain induced valley splitting for biaxially tensile strained Si and different field directions.

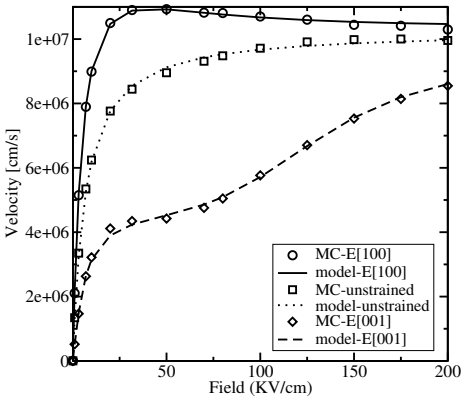

Figure 4: Electron velocity versus field characteristics for unstrained Si and strained Si on $Si_{0.6}Ge_{0.4}$.

field characteristics for unstrained Si and strained Si on $Si_{0.6}Ge_{0.4}$ as obtained from the MC simulations and from our model. Biaxial tensile strain increases (decreases) the in-plane (out-of-plane) electron velocity for the complete field range shown. Fig. 5 shows the velocity-field characteristics for a 1GPa uniaxially stressed Si layer for field along [110]. As can be seen, uniaxial compressive stress enhances the in-plane velocity in the same way as biaxial tensile strain.

INTERPOLATION

The velocity-field characteristics are extended to other field directions using a spherical harmonics interpolation. Designating the in-plane angle ϕ and the polar angle θ, and expanding up to 4^{th} order yields the velocity along an arbitrary field direction.

$$v(\theta,\phi) = a_{00}P_0^0(\chi) + a_{20}P_2^0(\chi) + a_{40}P_4^0(\chi) + a_{44}P_4^4(\chi)\cos(4\phi) \tag{3}$$

Here $\chi = \cos(\theta)$, a_{lm} denote the coefficients and P_l^m are the associated Legendre polynomials. We have chosen five field directions, [100], [110], [001], [101] and $[11\sqrt{2}]$ for our study. Solving exactly for the field directions [100], [110] and [001] while minimizing the error between field directions [101] and $[11\sqrt{2}]$, the four coefficients in (3) can be determined. Fig. 6 shows a comparison of the results obtained from the interpolation and from MC simulations for uniaxially stressed Si and the field along [211] direction.

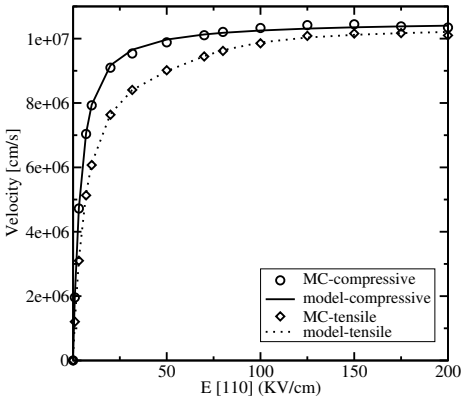

Figure 5: Electron velocity versus field characteristics for Si under uniaxial stress (1GPa) along [001] and field along [110].

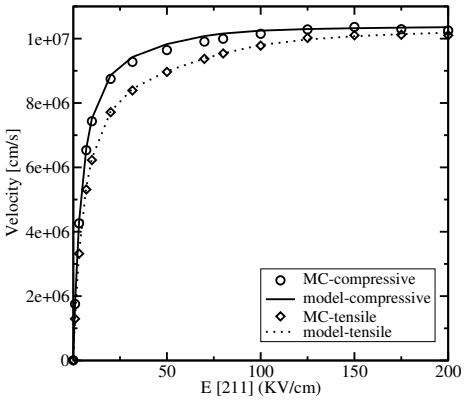

Figure 6: Electron velocity versus field characteristics for Si under uniaxial stress (1GPa) along [001] and field along [211].

CONCLUSIONS

The electron high-field transport in strained Si was studied for different field directions and stress/strain conditions. A phenomenological approach to describe the velocity-field characteristics for the longitudinal velocity component has been proposed. The analytical model shows good agreement with MC simulation results.

ACKNOWLEDGEMENT

This project has been supported in parts by the European Commission, NoE SINANO, IST-506844, and NoE TARGET, IST-1-507893.

REFERENCES

[1] K. Uchida *et al.*, "Experimental Study of Biaxial and Uniaxial Strain Effects on Carrier Mobility in Bulk and Ultrathin-Body SOI MOSFETs," in *IEDM Tech.Dig.*, 2004, pp. 229–232.

[2] A. Shimizu *et al.*, "Local Mechanical-Stress Control (LMC) : A New Technique for CMOS Performance Enhancement," in *IEDM Tech.Dig.*, 2001, pp. 433–437.

[3] S. Dhar *et al.*, "Electron Mobility Model for Strained-Si Devices," *IEEE Trans.Electron Devices*, vol. 52, no. 4, pp. 527–533, 2005.

[4] M. Rieger and P. Vogl, "Electronic-Band Parameters in Strained $Si_{1-x}Ge_x$ Alloys on $Si_{1-y}Ge_y$ Substrates," *Phys.Rev.B*, vol. 48, no. 19, pp. 14276–14287, 1993.

[5] Technische Universität Wien, Austria, *MINIMOS-NT 2.1 User's Guide*, 2004.